Int. J. Therm. Sci. (1999) 38, 305–314

An experimental study of the void fraction distribution in adiabatic water–air two-phase flows in an inclined tube

Klaus Spindler*, Erich Hahne

Institut für Thermodynamik und Wärmetechnik (ITW), Universität Stuttgart, Pfaffenwaldring 6, 70550 Stuttgart, Germany

(Received 15 June 1998, accepted 28 September 1998)

Abstract — A fibre optical probe is used to measure the radial distribution of void fraction and bubble frequency of adiabatic water–air two-phase flow in an inclined tube. Three typical void fraction distributions can be established for vertical two-phase flow: sliding bubble flow, coring bubble flow, and an intermediate type. These typical distributions are influenced by the angle of inclination in different ways. In case of coring bubble flow, the void fraction maximum near the tube axis moves to the upper part of the cross-section when the vertical tube changes to the horizontal position. In case of sliding bubble flow, one of the void fraction maxima near the tube wall is increased (upper part of cross-section) and the other one is decreased (lower part of cross-section) when the inclination changes from vertical to horizontal. The flow pattern transition can also be seen in the change of equivalent bubble diameters. © Elsevier, Paris.

two-phase flow / inclined tube / water-air / void fraction / bubble frequency / equivalent bubble diameter / fibre optical probe

Résumé — Étude expérimentale de la distribution de la fraction de vide dans des écoulements diphasiques adiabatiques eau-air en tube incliné. Une sonde à fibre optique a été utilisée pour mesurer la distribution radiale de la fraction de vide et la fréquence des bulles dans un écoulement diphasique adiabatique eau-air à l'intérieur d'un tube incliné. Trois distributions de fraction de vide typiques peuvent être définies pour l'écoulement diphasique vertical : bulles glissant le long de la paroi, bulles en écoulement central et cas intermédiaire. Ces distributions types sont influencées par l'inclinaison du tube. Dans le cas d'un écoulement central des bulles, le maximum de la fraction de vide, situé au voisinage de l'axe du tube, se déplace vers la partie supérieure d'une section transversale lorsque le tube passe de la position verticale à la position horizontale. Dans le cas de bulles glissant à la paroi, le maximum de la fraction de vide au voisinage de la paroi augmente (partie supérieure de la section) ou diminue (partie inférieure de la section) quand l'inclinaison varie de la position verticale à la position horizontale. La transition de la configuration de l'écoulement peut aussi être représentée par le changement des diamètres équivalents des bulles. © Elsevier, Paris.

écoulement diphasique / tube incliné / eau-air / fraction de vide / fréquence des bulles / diamètre équivalent des bulles / sonde à fibre optique

Nomenclature

d	inner tube diameter	m
D_B	bubble diameter	m
f_{loc}	local bubble frequency	s^{-1}
F_B	buoyancy force	N
F_D	drag force	N
F_L	lift force	N
r	radius	m
R	inner tube radius	m
r/R	dimensionless radial position	
w_B	bubble velocity	$m \cdot s^{-1}$
w_G	gas velocity	$m \cdot s^{-1}$
w_{G_0}	superficial gas velocity	$m \cdot s^{-1}$
w_{L_0}	superficial liquid velocity	$m \cdot s^{-1}$

Greek symbols

ε_{av}	cross-sectional average void fraction	%
ε_{loc}	local void fraction	%
ε_{max}	maximum void fraction	%
Φ	angle of inclination	°

* Correspondence and reprints.
pm@itw.uni-stuttgart.de

1. INTRODUCTION

Two-phase flow in inclined tubes is found in a number of technical applications. Oceanic pipelines have to be adjusted to fit the sea-bottom. In this case inclined sections of the pipeline occur automatically. Solar collectors have been developed for process heat production up to temperatures of about 150 °C (e.g. [1]). Boiling water is used as working fluid in order to achieve high system efficiencies. The tilt of the boiler tubes corresponds to the degree of latitude of the system location. Another application is the two-phase flow in the absorber tube of a concentrating parabolic trough collector with direct steam generation in solar power plants [2]. Boiling water, instead of heat transfer oil, is used as working fluid in the absorber tube. In order to reduce the cosine losses, the angle of inclination of the parabolic trough system is about 10°. To avoid a large height at the northern end of the trough system, it must be divided into single elements resulting in a saw-tooth arrangement. On account of the high heat flux on half of the outer tube perimeter, the heat transfer inside the tube must be uniformly high on the corresponding inner surface. Otherwise, high local wall temperatures will occur as shown by Heidemann et al. [3]. This will cause thermal stress and deformation of the tube. A uniformly high heat transfer coefficient inside can be achieved by sufficient wetting of the total inner surface with liquid. This is affected by the void fraction distribution and the two-phase flow pattern.

2. LITERATURE

Most of the work on two-phase flow in inclined tubes has been done with adiabatic two component systems water–air [4] or oil–air [10–13]. Transparent tubes were used for visual observation of the flow pattern and flow pattern transitions.

Beggs and Brill [14] found that the liquid hold-up in inclined two-phase flow reaches a maximum (i.e. minimum in void fraction) at an angle of inclination of approximately 50° from horizontal. This phenomenon may be explained by considering the effects of gravity and viscosity on the liquid phase. As the angle of the tube is increased from the horizontal, gravity forces acting on the liquid cause a decrease of liquid velocity, thus increasing slip and liquid hold-up. As the angle is increased further, the liquid bridges the entire tube, reducing slip between phases and thus decreasing hold-up. This fact is confirmed by a maximum of the bubble propagation velocity at angles of inclination between 30° and 60° [15–17]. The fact that liquid hold-up is the same at angles of 90° and 20° explains why vertical hold-up correlations can be used successfully for horizontal flow. Lo [18] reported an increase in void fraction (i.e. decrease in liquid hold-up) with an angle of inclination increasing from 45° to 90°. The effect is greater at higher gas flow rates.

The void fraction or the liquid hold-up, determined from pressure drop measurements (e.g. [18, 19]), represents the global void fraction in a certain part of the inclined tube. Local void fraction measurements across the flow cross-section are not given in the literature for inclined tubes.

A few experimental studies on flow boiling in inclined tubes are reported in the literature [20–26]. Krishna [20] found that in bubbly or intermittent flow, the heat transfer coefficient passed through a minimum with an increasing angle of inclination. In annular flow, the inclination has no significant effect on the heat transfer. Morcos et al. [27] found an optimum value of the heat transfer coefficient at an angle of inclination equal to 30°. Fedorov and Klimenko [22] showed that the local heat transfer coefficient depends on the orientation of the channel. The heat transfer coefficient in the upper circumference of the channel showed a somewhat weaker dependency on the heat flux than in the lower circumference. This effect is obviously connected to the asymmetry of two-phase flow structure. Simon [25] performed experiments with water/steam two-phase flow in a stainless steel tube (inner diameter 15.7 mm, length 5 m) at pressures up to 100 bar, mass fluxes between 70 and 280 $kg \cdot s^{-1} \cdot m^{-2}$ and heat fluxes up to 100 $kW \cdot m^{-2}$. The angle of inclination was varied between 0° and 45°. Flow patterns were detected using an optical system. The flow pattern changes at angles between 0.1° and 0.4° from stratified to slug flow. The slug frequencies increase with increasing angles of inclination. A new flow pattern map using a modified Froude number and a dimensionless parameter containing the vapour mass quality and the density ratio of vapour and liquid was presented. Hahne et al. [26] studied the effect of tilt on flow patterns of water/steam flow in a heated tube (inner diameter 23.4 mm, length 8 m) at pressures up to 100 bar and tube inclinations of 0°, 4° and 8°. The results show that the minimum mass flow required to avoid stratified flow increases with pressure and heat flux, but decreases strongly with upward tilt.

The mechanism of boiling heat transfer in inclined channels is closely related to the distribution of the liquid and vapour phases, as well as the flow pattern. Therefore, in order to identify the flow boiling heat transfer phenomena, it is necessary to know the local two-phase flow conditions at different angles of inclination.

3. EXPERIMENTAL SET-UP

3.1. Two-phase flow loop

As a first step we started to study the adiabatic two-phase flow. Water and air were chosen because of easy

handling and the inexpensive components of the test facility. A flow loop was built with two transparent test tubes of different diameter (30 mm outer diameter and 4 mm wall thickness; 20 mm outer diameter and 3 mm wall thickness) to study the local structure of two-phase flow in inclined tubes. The inner diameters of the acrylic resin tubes are 22 mm and 14 mm, respectively. The length of the test section is 4 000 mm. The angle of inclination can be adjusted continuously between 0° (horizontal) and 90° (vertical). A schematic diagram of the experimental apparatus is shown in *figure 1*. Water and pressurized air are mixed together using static mixing devices (Sulzer mixer SMV-DN 15, SMV-DN 25). Pressurized air is blown into the flowing water through four capillary tubes before entering the mixing device. The mixer itself consists of five mixing elements arranged in series within a tube. Each element consists of corrugated plates which are arranged to form open intersecting channels. In these channels, the fluid flow is split into sub-flows, which are repeatedly redirected and re-united, thereby achieving intermixing in the radial direction. This results in a uniform distribution of the void fraction over the whole flow cross-section [28]. The two-phase mixture flows up in an inclined acrylic resin tube. The air can leave the loop in the upper plenum, and only water flows back. The temperature of the water is kept constant by a water-cooled heat exchanger. The flow rate of water and air is adjustable and is measured by flowmeters.

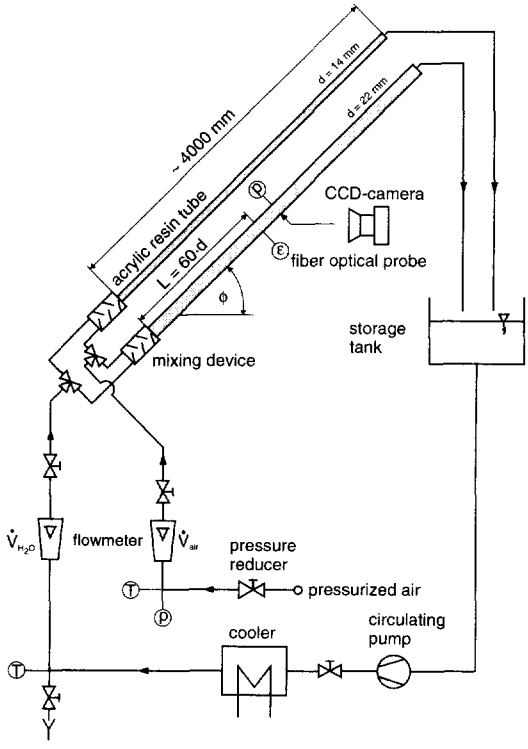

Figure 1. Experimental set-up of the two-phase flow loop.

3.2. Fibre optical system

Local void fraction measurements are performed with a fibre optical probe. The geometry of the optical probe is shown in *figure 2*. For easy installation a straight form is used. The optical fibre (200 µm/230 µm core/clad diameter, multimode, step-index profile) is ground at its tip to a cone with a 90° angle. For protection the fibre is glued concentrically into stainless steel tubes. The inner one surrounding the fibre has a diameter of 0.5 mm to provide stiffness. Thus the sensitive diameter of the optical probe is 0.5 mm. A larger diameter (3.0 mm) outer tube serves to further stiffen the probe and connect it to the positioning system shown in *figure 3*. The probe can be positioned along the tube diameter from bottom to top of the cross-section with high accuracy using a micrometer screw. Its position can be checked while the probe tip is positioned exactly in the tube centreline by looking through two diametrically opposed gaps in the clamping device.

Figure 4 shows the schematic arrangement of the fibre optical measuring system. IR-light is sent continuously from the optical emitter into the optical fibre. It leaves at its tip as long as liquid covers it. When gas hits the tip, the light is totally reflected back into the fibre. This reflected light passes an optical coupler. The optical detector converts the light into electrical signals. These are amplified and transformed into digital signals when the trigger level is reached. The local void fraction

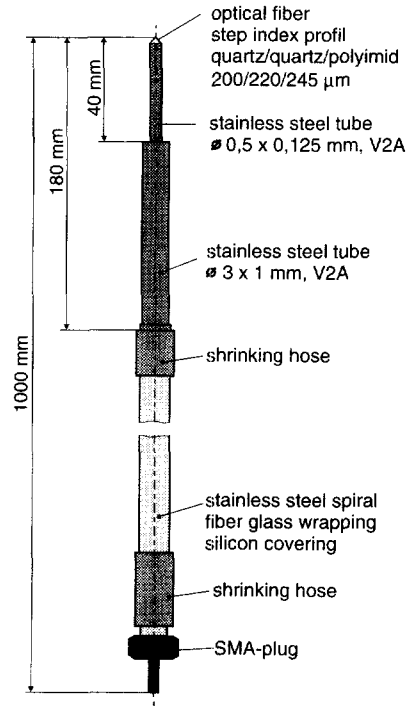

Figure 2. Fibre optical probe.

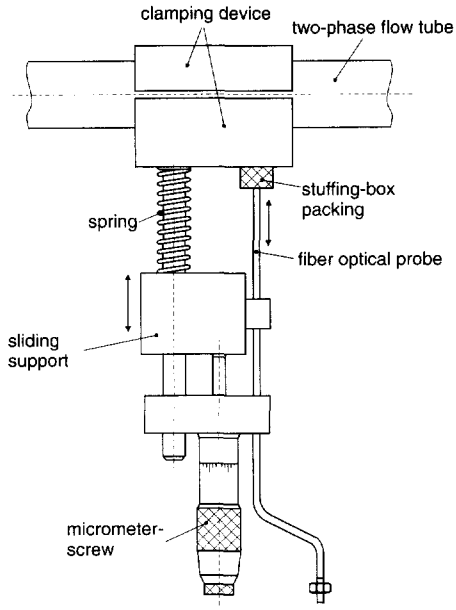

Figure 3. Positioning system for the fibre optical probe.

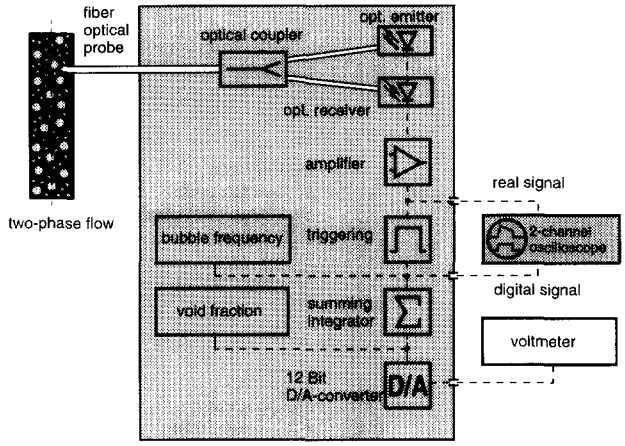

Figure 4. Fibre optical electronic equipment.

is obtained by summing up the duration of all these digital signals and dividing by the integration time. The integration time is set to 1 s. With an external voltmeter, the void fraction signal is measured over 20 s, 5 times at each measuring point. The average values are presented in the *figures*. The bubble frequency is obtained by counting the digital signals. Detailed descriptions of the optical probe, the signal processing and the measuring accuracy are given by Spindler et al. [29] and Spindler [30]. The integrated void fraction profiles measured by the fibre optical probe show mean deviations of about -20 % and maximum deviations of about -40 % compared with the global void fraction measured by a γ-densitometer.

3.3. Video system

In addition, pictures of the two-phase flow were taken using a video system. The optical arrangement is shown schematically in *figure 5*. All optical elements were fixed to the tube. Stroboscopic lightning in connection with a CCD camera (Pulnix TM 765) with an electronic shutter (1/10 000 s) was used to achieve focused pictures. A ground-glass plate was placed between the tube and the camera. The pictures supplied by the video recorder (Panasonic AG 4700) were analysed in a freezed frame mode and in slow motion to identify the two-phase flow pattern.

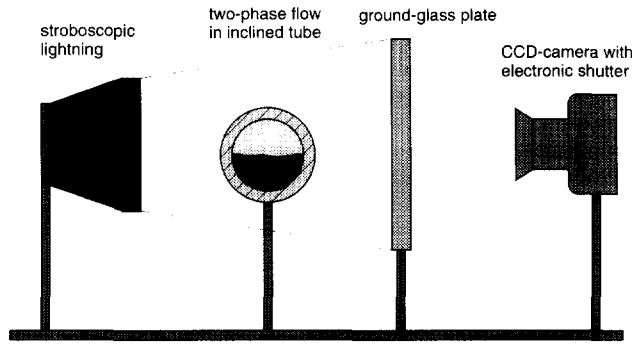

Figure 5. Optical arrangement for taking video pictures.

3.4. Experimental procedure and parameters

The temperature of the two-phase flow was kept constant at about 25 °C. The pressure in the test section was close to the ambient pressure. The superficial velocity of water and air and the angle of inclination were varied so that dispersed bubble flow, slug flow and stratified wavy flow could be observed. The radial distributions of void fraction and bubble frequency were measured diametrically from bottom to top of the cross-section. In total, 23 measuring positions were chosen. The distance between two positions is 1 mm with the exception of the wall region. The closest distance to the tube wall for which measurements were still feasible was 0.5 mm. The integration time was 20 s for each point. The optical probe was located at a distance of 60 diameters (inner tube diameter 22 mm) downstream of the mixing chamber.

The *table* shows the superficial velocity combinations for water (w_{L_0}) and air (w_{G_0}) which were studied. A comparison with the flow pattern map for vertical two-phase flow by Govier et al. [31] and the flow pattern map for horizontal two-phase flow by Baker [32] indicate that all points are situated in the slug flow region.

TABLE
Superficial velocity combinations.

		w_{L_0} (m·s^{-1})		
		0.75	1.0	1.5
w_{G_0} (m·s^{-1})	0.5	s	s	s
	1.0	i	i	s
	1.3	c	c	c

s: sliding bubble flow (ε_{max} near the tube wall); c: coring bubble flow (ε_{max} near the tube axis); i: intermediate type.

An equivalent bubble diameter D_B could be calculated assuming spherical bubbles:

$$D_B = \frac{3}{2} w_B \frac{\varepsilon_{loc}}{f_{loc}}$$

with local void fraction ε_{loc} and the local bubble frequency f_{loc}. The velocity of the bubbles is assumed to be $w_B = w_G = w_{G_0}/\varepsilon_{av}$. The average void fraction ε_{av} is obtained by integration of the local void fraction over the cross-section. For the vertical tube, this integration is performed over concentric annuli; for the inclined and the horizontal tube, this is done over chordal sections.

4. MOTION OF BUBBLES IN INCLINED TUBES

In vertical tubes, the transition from bubble to slug flow takes place when the void fraction reaches values of about 25 %. In inclined tubes, bubble flow no longer exists when the tube is inclined below a specific angle. This can be explained by the fact that decreasing the angle of inclination causes the bubbles to migrate to the upper pipe wall. This results in a high local void fraction there. Transition to slug flow takes place even when the cross-sectional average void fraction is less than 25 %. However, the transition may occur at a higher void fraction (possibly as high as 60 %) if coalescence is prevented, see [33].

The forces acting on a spherical bubble are shown in *figure 6*: the buoyancy force F_B, the drag force F_D and the lift force F_L. When the tube is slightly inclined the buoyancy force can be split into a radial component normal to the tube axis F_{Br} and an axial component parallel to the tube axis F_{Ba}. F_{Br} tends to keep the dispersed bubbles at the upper half of the cross-section and enhances the transition to slug flow. On the other hand, the lift force F_L tends to disperse the bubbles, maintaining the bubble flow pattern. Sometimes a zig-zag path of bubbles could be observed in the video pictures, while the bubbles move away from the pipe

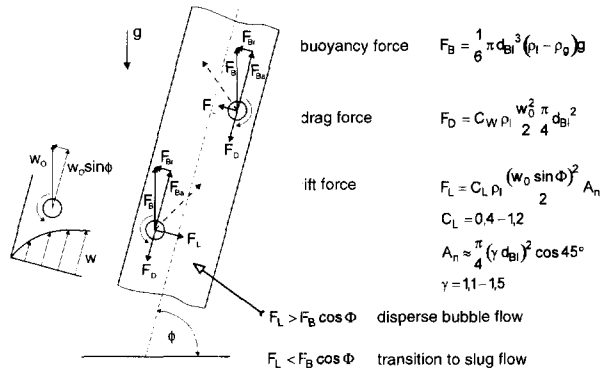

Figure 6. Forces acting on bubbles in inclined tubes.

crown towards the tube axis and then back to the upper part of the tube.

5. RESULTS

The radial distributions of measured void fraction, bubble frequency and calculated equivalent bubble diameter are shown in *figures 7* to *9* for seven angles of inclination: 0° (horizontal), 15°, 30°, 45°, 60°, 75° and 90° (vertical) for the tube with 22 mm inner diameter.

Because of the non-axisymmetrical distributions, the measurements had to be taken along the diameter from bottom to top of the cross-section. The dimensionless radial position r/R (inner tube radius R) starts at $r/R = -1$ (bottom of the cross-section for horizontal and inclined tube) up to $r/R = +1$ (top of the cross-section). The tube axis is represented by $r/R = 0$.

For vertical two-phase flow, three typical types of flow can be established [29]: sliding bubble flow, coring bubble flow and an intermediate type. Sliding bubble flow is characterised by an increase in void fraction near the tube wall. It is found if the superficial velocity of water is higher than that of air: see the *table*. In the opposite case (lower superficial velocity of water), coring bubble flow is detected with a void fraction maximum near the tube axis.

The typical void fraction distributions are influenced by the angle of inclination in a different manner. In case of sliding bubble flow, one void fraction maximum is increased (upper part of the cross-section for inclined tube) and the other maximum is decreased (lower part of the cross-section), when the inclination changes from vertical to horizontal: see *figure 7a*. The behaviour of the bubble frequency distribution is quite similar: see *figure 7b*. The flow pattern transition (from dispersed bubble, through elongated bubble, to stratified wavy flow) can also be seen in changing equivalent bubble diameter: see *figure 7c*. In case of coring bubble flow, the void fraction maximum near the tube axis moves to the top of the pipe when changing from vertical to horizontal tube direction: see *figure 8a*.

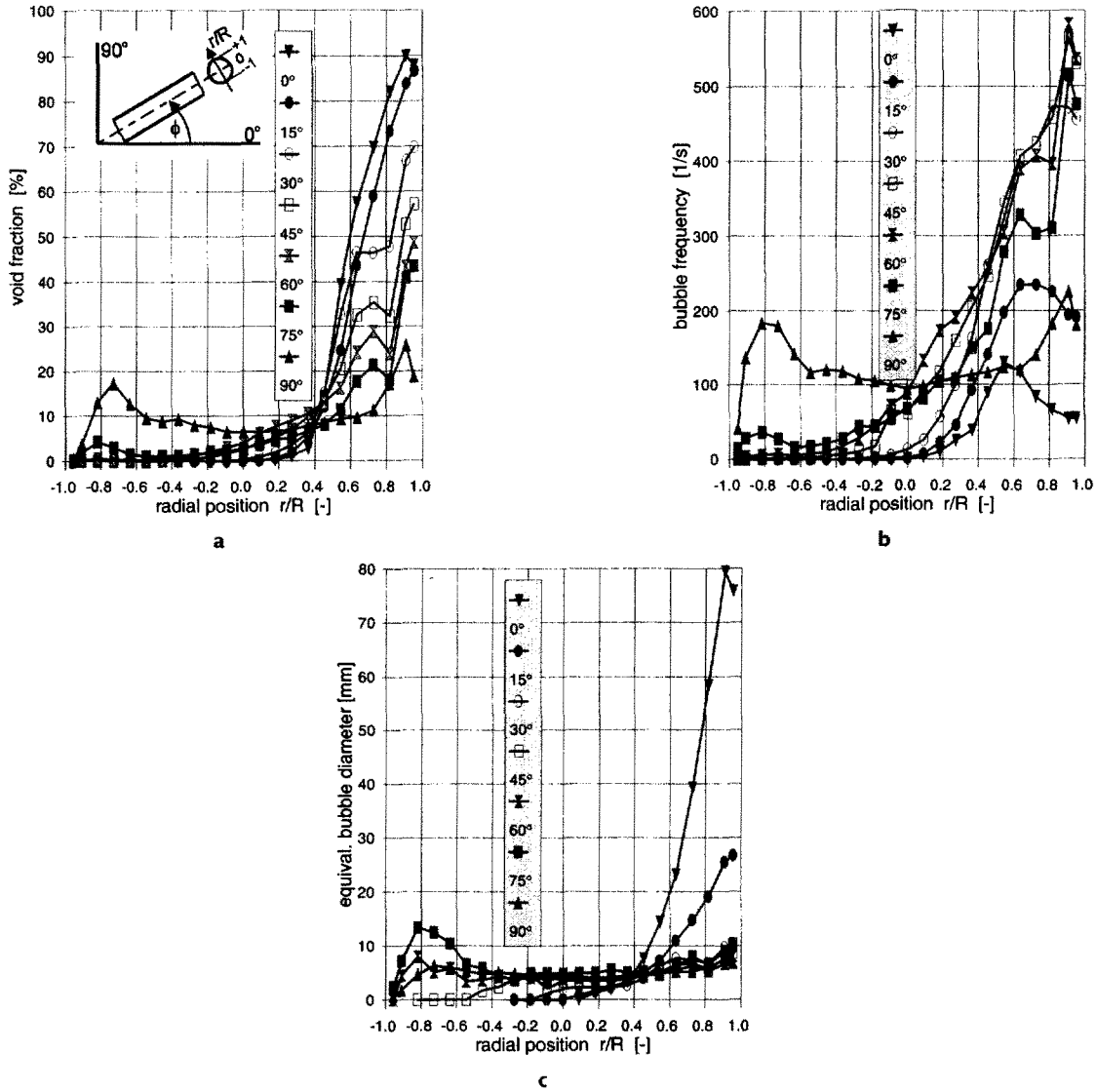

Figure 7. a. Radial distributions of void fraction at $w_{L_0} = 1.0$ m·s^{-1} and $w_{G_0} = 0.5$ m·s^{-1} (sliding bubble flow). **b.** Radial distributions of bubble frequency at $w_{L_0} = 1.0$ m·s^{-1} and $w_{G_0} = 0.5$ m·s^{-1}. **c.** Radial distributions of equivalent bubble diameter at $w_{L_0} = 1.0$ m·s^{-1} and $w_{G_0} = 0.5$ m·s^{-1}.

Figures 7a and *7b* show that the maximum in void fraction and bubble frequency for the vertical tube (90°) at $r/R = 0.9$ increases rapidly with decreasing inclination. The local void fraction reaches a maximum of 90 % at $r/R = 0.9$ for the horizontal tube (0°). The maximum of the local bubble frequency is found for angles of inclination of about 30° and 45° at $r/R = 0.9$. The maximum values measured are about 600 s^{-1}. The maximum of the void fraction and bubble frequency at $r/R = -0.7$ decreased instantly when the tilt of the tube deviates from the vertical direction. Bubbles from the lower part of the cross-section ($r/R < 0$) are moving to the upper part ($r/R > 0$). A sharp drop in the bubble frequency is found for angles of inclination smaller than 30° in the region $r/R > 0.5$ (*figure 7b*). Due to an increasing void fraction and a decreasing bubble frequency in the upper part of the cross-section ($r/R > 0.5$), the equivalent bubble diameter (*figure 7c*) grows rapidly. This indicates slug flow when an inclination of 15° is reached. The slug length is between 20 and 80 mm. These slugs appear in the cross-section between $0.2 < r/R < 1$. The region $r/R < 0.2$ is fully covered by the liquid.

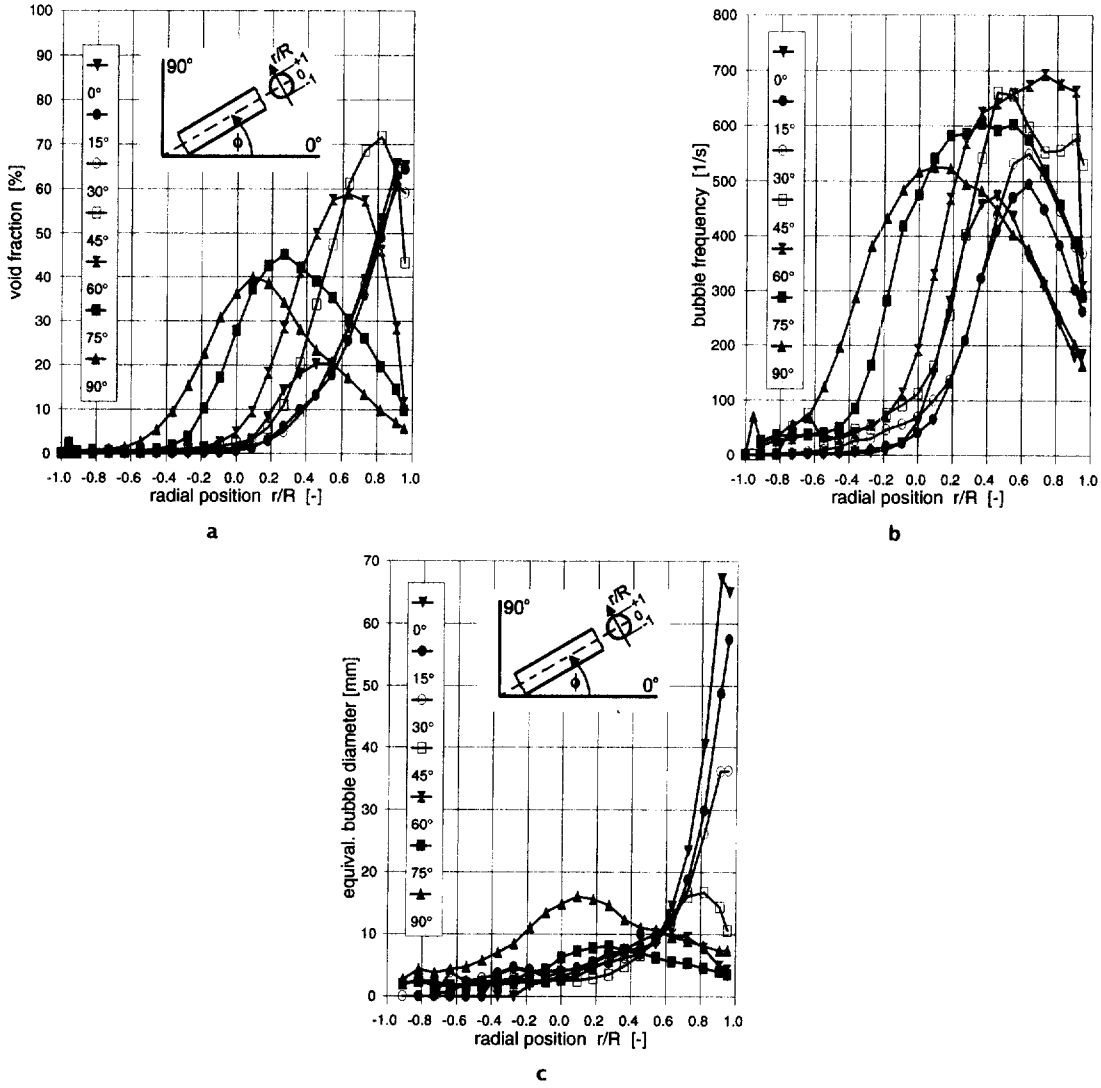

Figure 8. a. Radial distributions of void fraction at $w_{L_0} = 1.5$ m·s^{-1} and $w_{G_0} = 1.3$ m·s^{-1} (coring bubble flow). **b.** Radial distributions of bubble frequency at $w_{L_0} = 1.5$ m·s^{-1} and $w_{G_0} = 1.3$ m·s^{-1}. **c.** Radial distributions of equivalent bubble diameter at $w_{L_0} = 1.5$ m·s^{-1} and $w_{G_0} = 1.3$ m·s^{-1}.

Figures 8a and *8b* show that the maximum in void fraction and bubble frequency near the tube centreline ($r/R = 0$) for the vertical tube moves rapidly to the upper part of the cross-section ($r/R \geq 0$) with decreasing inclination. The bubble frequency increases until an inclination of 60° is reached, then it decreases rapidly for lower inclinations. This results in an increase of the equivalent bubble diameter in the region $r/R > 0.5$ for inclinations lower than 60°: see *figure 8c*.

A superposition of the effects mentioned above is seen in the *figures 9a*, *9b* and *9c*. The maximum of void fraction and bubble frequency at $r/R = -0.7$ decreases, and the maximum at $r/R = 0$ is shifted to greater r/R-values with decreasing inclination. This yields a strong increase of the equivalent bubble diameter in the region $r/R > 0$ (upper half of the tube cross-section) for inclinations of less than 45°: see *figure 9c*.

Corresponding to Beggs and Brill [14], it was found that the average void fraction generally decreases with increasing inclination, except for a high superficial gas velocity $w_{G_0} = 1.3$ m·s^{-1}. The average void fraction for horizontal two-phase flow (0°) is approximately the same as for vertical two-phase flow (90°).

An effect of the entrance length could not be clearly seen in the void fraction profiles measured additionally at $L/d = 30$ and 40. But there is an effect with increasing flow length, which can be seen in the video pictures taken at $L/d = 25$ and 120: see *figures 10a* and *10b*.

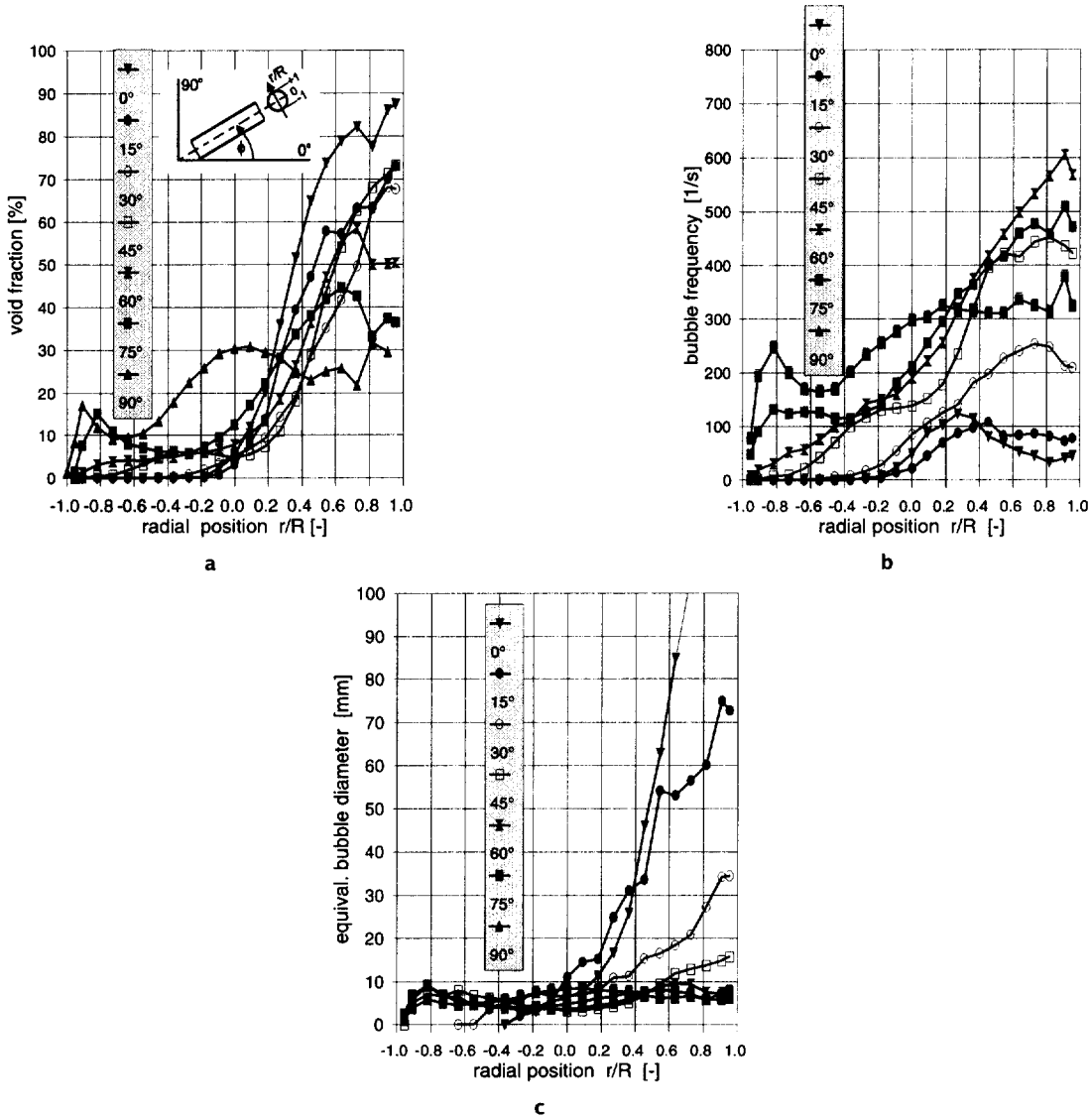

Figure 9. a. Radial distributions of void fraction at $w_{L_0} = 0.75$ m·s^{-1} and $w_{G_0} = 1.0$ m·s^{-1} (intermediate type). **b.** Radial distributions of bubble frequency at $w_{L_0} = 0.75$ m·s^{-1} and $w_{G_0} = 1.0$ m·s^{-1}. **c.** Radial distributions of equivalent bubble diameter at $w_{L_0} = 0.75$ m·s^{-1} and $w_{G_0} = 1.0$ m·s^{-1}.

The pictures of the two-phase flow had been taken for the fixed superficial water velocity $w_{L_0} = 0.8$ m·s^{-1} and four superficial air velocities $w_{G_0} = 0.1$, 0.5, 1.0 and 2.5 m·s^{-1}. At $L/d = 25$ (left hand side of *figure 10a* and *10b*), a lot of small bubbles can be seen among larger bubbles. The bubbles coalesce more and more with increasing flow length $L/d = 120$ (right hand side of *figures 10a* and *10b*). The smaller bubbles disappeared. The slug length is also increased at $L/d = 120$. The front end of the slug is deformed due to drag forces. Small bubbles are flowing behind the slugs. At the high superficial gas velocity $w_{G_0} = 2.5$ m·s^{-1}, the interface between liquid and gas is very wavy. A lot of small bubbles can be seen near the interface at $L/d = 0.25$ (left hand side of *figures 10a* and *10b*). The number of bubbles near the gas-liquid interface decreased strongly at $L/d = 120$ (right hand side of *figures 10a* and *10b*).

6. CONCLUSIONS

The radial distribution of local void fraction and bubble frequency in inclined two-phase flow is strongly influenced by the angle of inclination. As the vertical

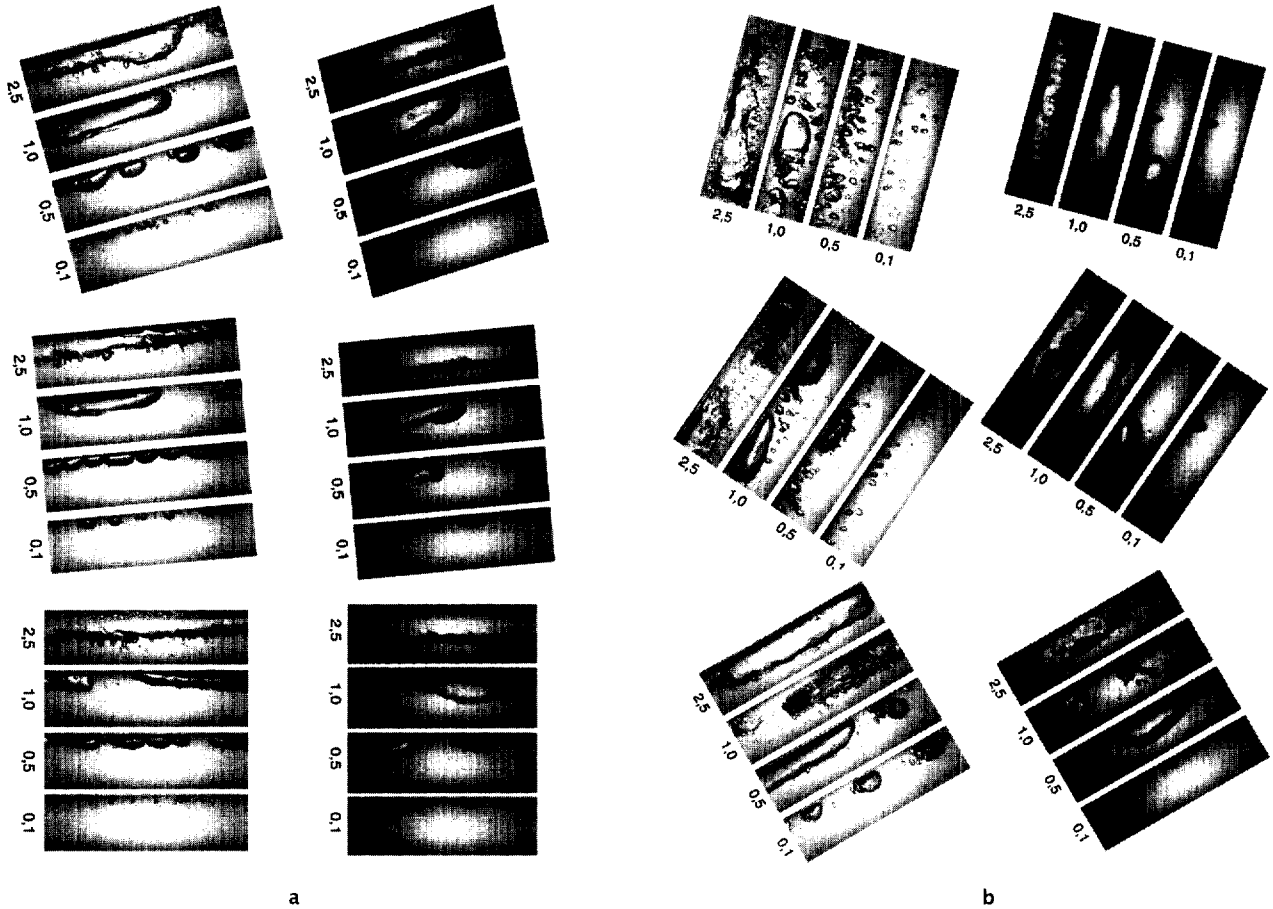

Figure 10. a. Pictures of the two-phase flow ($w_{L_0} = 0.8$ m·s^{-1}; $w_{G_0} = 0.1$, 0.5, 1.0 and 2.5 m·s^{-1}) at positions $L/d = 25$ (left hand side) and $L/d = 120$ (right hand side) for angles of inclination 0°, 5° and 15°. **b.** Pictures of the two-phase flow ($w_{L_0} = 0.8$ m·s^{-1}; $w_{G_0} = 0.1$, 0.5, 1.0 and 2.5 m·s^{-1}) at position $L/d = 25$ (left hand side) and $L/d = 120$ (right hand side) for angles of inclination 30°, 60° and 75°.

tube is inclined, the bubbly flow pattern disappears because of high local concentrations of voids at the upper part of the cross-section. The flow pattern transitions can be seen in changing equivalent bubble diameters. For the vertical two-phase flow, a maximum in the void fraction profile appears in the tube axis for $w_{G_0} > w_{L_0}$. For $w_{L_0} > w_{G_0}$, a void fraction maximum near the tube wall is found. For the inclined tube, all gas is in the upper part of the cross-section for $0.75 < w_{L_0}/w_{G_0} < 1.15$ and angles of inclination $\Phi < 45°$. At $w_{L_0}/w_{G_0} = 2$, this occurs already for $\Phi < 30°$. In spite of recent advances, there is much further work to be done on the subject of two-phase flow in inclined tubes in general, and on flow boiling in inclined tubes in particular, in order to analyse the local flow conditions for flow pattern transitions. The experimental data can be used for the validation of two-phase computer codes. The effect of flow length must be considered due to coalescence effects.

REFERENCES

[1] Benz N., Direkte solarthermische Prozeßdampferzeugung in evakuierbaren Flachkollektoren, VDI Fortschrittsberichte, Reihe 6, Nr. 311, VDI Verlag, Düsseldorf, 1994.

[2] Müller M., How to master the DSG process? Some open questions, in: Proc. 5th Sde Boker Symposium on Solar Electricity Production, Israel, 1993, pp. 203–235.

[3] Heidemann W., Spindler K., Hahne E., Steady-state and transient temperature field in the absorber tube of a direct steam generating solar collector, Int. J. Heat Mass Trans. 35 (1992) 649–657.

[4] Barnea D., Shoham O., Taitel Y., Dukler A.E., Flow pattern transition for gas–liquid flow in horizontal and inclined pipes. Comparison of experimental data with theory, Int. J Multiphas. Flow 6 (1980) 217–225.

[5] Weisman J., Kang S.Y., Flow pattern transition in vertical and upwardly inclined lines, Int. J. Multiphas. Flow 7 (1981) 271–291.

[6] Spedding P.L., Chen J.J.J., Nguyen V.T., Pressure drop in two phase gas-liquid flow in inclined pipes, Int. J. Multiphas. Flow 8 (1982) 407–431.

[7] Johnston A.J., Two-Phase Stratified Flow in Inclined Pipes, Mech. Eng. Trans.-Inst. Engineers Australia 10 (2) (1985) 75–80.

[8] Andreussi P., Bendiksen K., An investigation of void fraction in liquid slugs for horizontal and inclined gas-liquid flow, Int. J. Multiphas. Flow 15 (1989) 937–946.

[9] Wood D.G., The effect of inclination on flow regime boundaries and slug flow characteristics, J. Energ. Resour.-ASME 111 (1989) 181–186.

[10] Stanislav J.F., Kokal S., Nicholson M.K., Intermittent gas-liquid flow in upward inclined pipes, Int. J. Multiphas. Flow 12 (1986) 325–335.

[11] Stansilav J.F., Kokal S., Nicholson M.K., Gas-liquid flow in downward and upward inclined pipes, Can. J. Chem. Eng. 64 (6) (1986) 881–890.

[12] Kokal S.L., Stanislav J.F., An experimental study of two-phase flow in slightly inclined pipes. I. Flow patterns, Chem. Eng. Sci. 44 (3) (1989) 665–679.

[13] Kokal S.L., Stanislav J.F. An experimental study of two-phase flow in slightly inclined pipes. II. Liquid holdup and pressure drop, Chem. Eng. Sci. 44 (3) (1989) 681–693.

[14] Beggs H.D., Brill J.P., A study of two-phase flow in inclined pipes, J. Petrol. Technol. 25 (1973) 607–613.

[15] Zukoski E.E. Influence of viscosity, surface tension, and inclination angle on motion of long bubbles in closed tubes, J. Fluid Mech. 25 (4) (1966) 821–837.

[16] Bendiksen K.H., An experimental investigation of the motion of long bubbles in inclined tubes, Int. J. Multiphas. Flow 10 (1984) 467–483.

[17] Weber M.E., Alarie A., Ryan M.E., Velocities of extended bubbles in inclined tubes, Chem. Eng. Sci. 41 (9) (1986) 2235–2240.

[18] Lo S.M., Development of a new interphase friction law for air-water flows in inclined pipes, Ph.D. Thesis, CFDU/85/14, Imperial College of Science and Technology, London, 1985.

[19] Hasan A.R., Kabir C.S., Two-phase flow in vertical and inclined annuli, Int. J. Multiphas. Flow 18 (1992) 279–293.

[20] Krishna M.M., Studies on two-phase flow and boiling heat transfer in inclined tubes with reference to solar collectors, Ph.D. Thesis, IIT Kanpur, India, 1985.

[21] Krishna M.M., Rao D.P., Studies on flow boiling in an inclined tube with reference to solar collectors, in: Proc. 9th Biennial Congress of the Int. Sol Energy Society, INTERSOL 85, Pergamon Press, New York, USA, 1986, pp. 1368–1372.

[22] Fedorov M.V., Klimenko V.V., The effect of orientation of a channel heat transfer with forced two-phase flow of nitrogen, Thermal Engineering 35 (1988) 347–349.

[23] Müller M., Lippke F., Ratzesberger R., Direct steam generation in parabolic-trough solar power plants: a resume on issues learned and an outlook on the next steps, in: Proc. ISES Solar World Congress, Budapest, 1993, pp. 203–208.

[24] Müller M., Strömungsphänomene bei der Direktverdampfung in Parabolrinnen-Solarkraftwerken, VDI Fortschrittsberichte, Reihe 6, Nr. 335, VDI Verlag, Düsseldorf, 1995.

[25] Simon M., Experimentelle Untersuchungen zu Strömungsformen in horizontalen und geneigten Verdampferrohren, Forschungszentrum Karlsruhe, Bericht FZKA 5950, 1997.

[26] Hahne E., Herrmann U., Rheinländer J., The effect of tilt on flow patterns of water/steam flow through heated tubes, in: Proc. 4th World Conference on Experimental Heat Transfer, Fluid Mechanics and Thermodynamics, Brussels, 1997, pp. 925–934.

[27] Morcos S.M., Mobarak A., Hilal M., Mohareb M.R., Boiling heat transfer in horizontal and inclined rectangular channels. J Heat Trans.-T. ASME 109 (1987) 503–508.

[28] Schneider G., Static mixers as gas/liquid reactors, in: Fluid Mixing IV, Institution of Chemical Engineers, Sympos. Series No. 121, EFCE Event No. 432, 1990, pp. 109–119.

[29] Spindler K., Bierer M., Lorenz G., Erhard A., Hahne E., Measurements in vertical gas-liquid two-phase flows using an optical fiber probe, in: Proc. 1st World Conference on Experimental Heat Transfer, Fluid Mechanics and Thermodynamics, Dubrovnik, 1988, pp. 348–357.

[30] Spindler K., Untersuchung zum Mischereinfluß auf die lokale Struktur einer adiabaten Zweiphasenströmung mit einem faseroptischen sensor, Ph.D. Thesis, University of Stuttgart, 1989.

[31] Govier G.W., Radford B.A., Dunn J.S.C., Short W.L., The upwards vertical flow of air-water mixtures, Can. J. Chem. Eng. 36 (1958) 195–202.

[32] Baker O., Simultaneous flow of oil and gas, Oil Gas J. 53 (12) (1954) 184–195.

[33] Whalley P.B., Two-Phase Flow and Heat Transfer, Oxford Chemistry Primers 42, Oxford Univ Press, New York, 1996.